Electronic Supplementary Material (ESI) for Inorganic Chemistry Frontiers.

Supporting Information

***Meso*-aryl substituents modify the electrochemical profile and palladium(II) coordination of redox-active tripyrrin ligands**

Iva Habenšus and Elisa Tomat*

Contents *page*

Spectroscopic and electrochemical characterization of ligands (Figs. S1-S5) S2

Spectroscopic characterization of complexes (Figs. S6-S10) S6

X-ray diffraction analysis (Figs. S11-S14, Tables S1-S2) S10

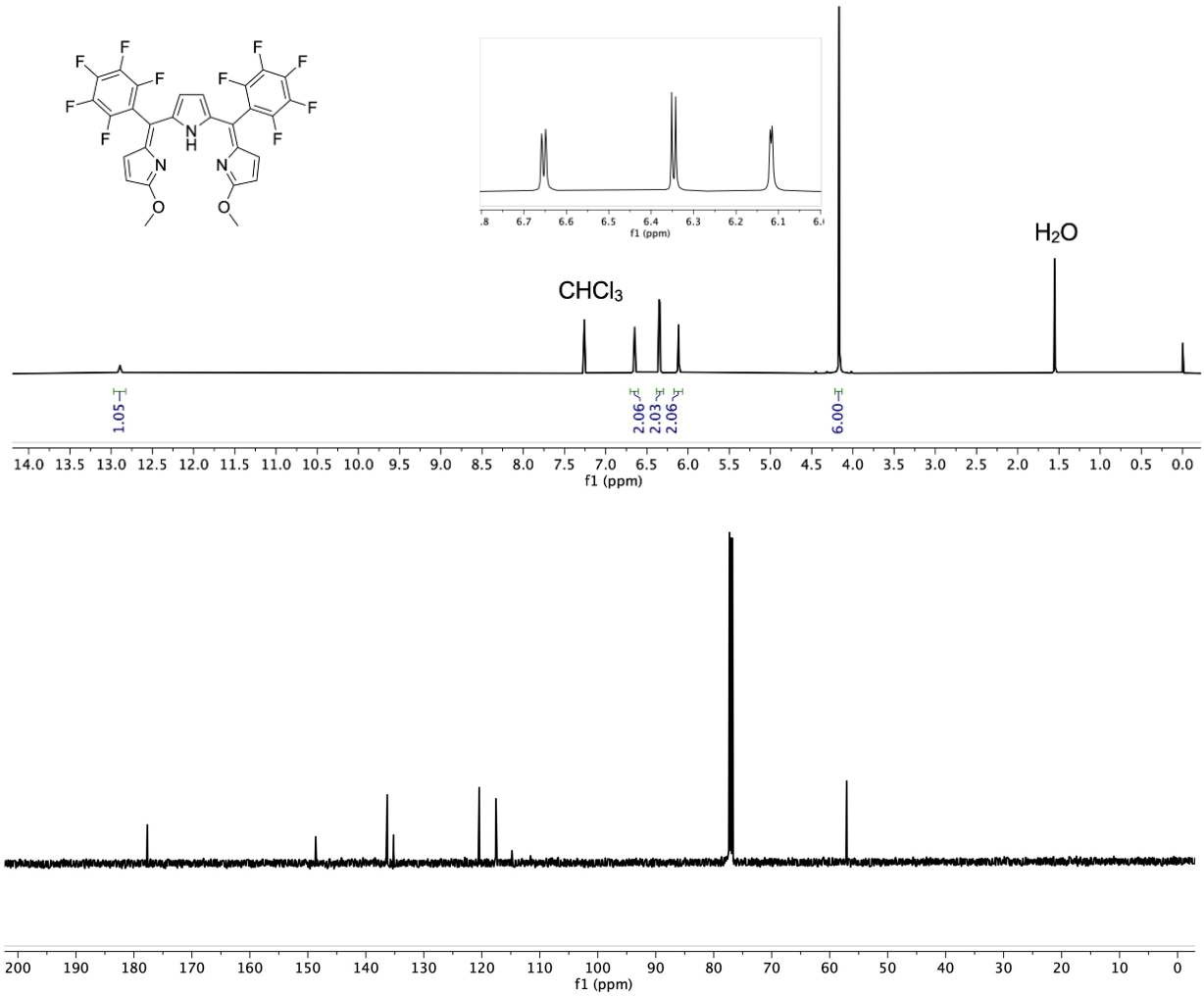

Fig. S1. ^{1}H NMR (top) and ^{13}C NMR (bottom) spectra of HTM_{C6F5} in $CDCl_3$ at room temperature.

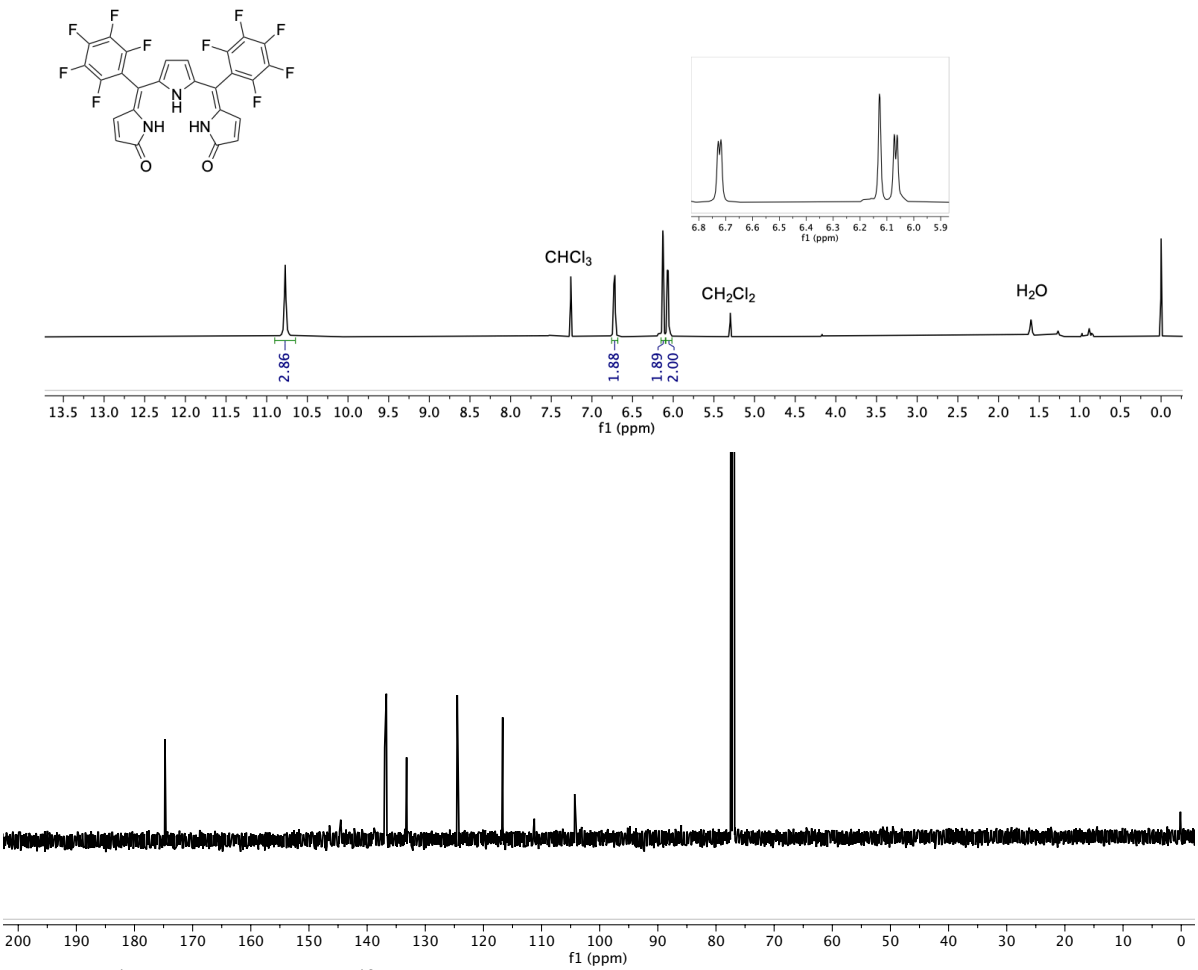

Fig. S2. ^{1}H NMR (top) and ^{13}C NMR (bottom) spectra of H_3TD_{C6F5} in $CDCl_3$ at room temperature.

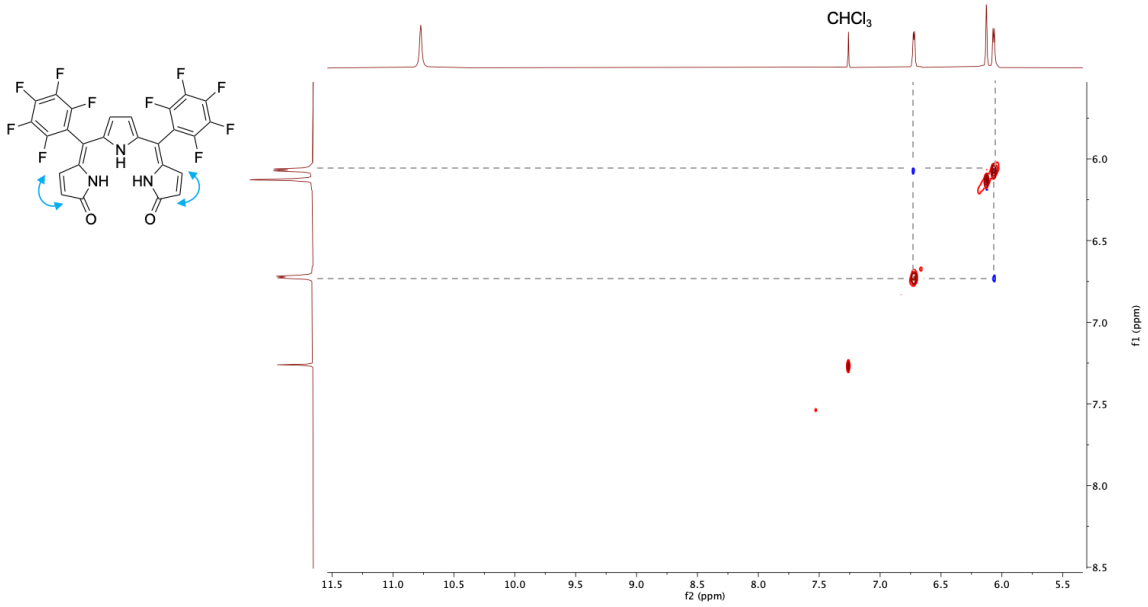

Fig. S3. NOESY NMR spectrum of *meso*-pentafluorophenyltripyrrindione (H_3TD_{C6F5}) in $CDCl_3$.

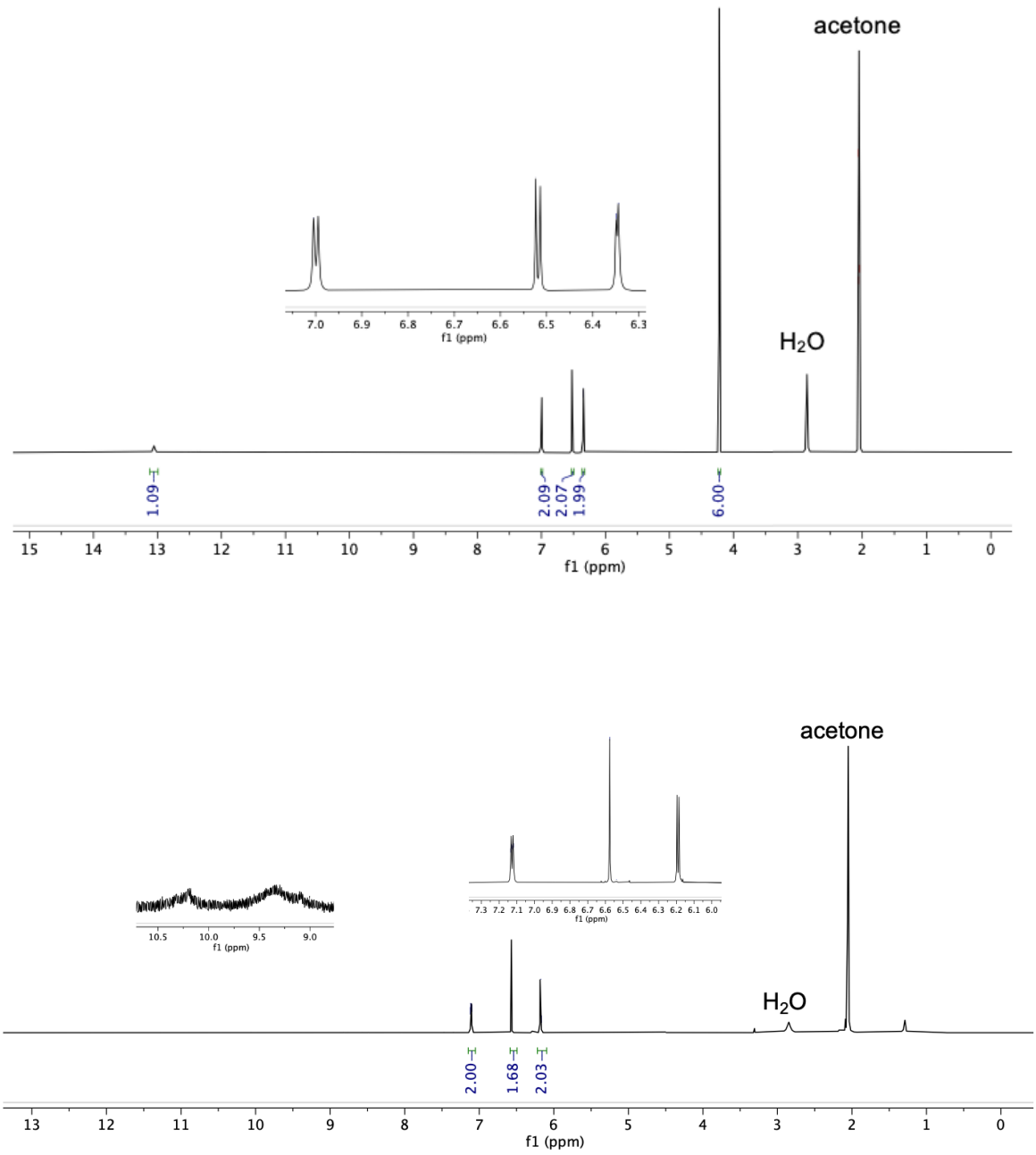

Fig. S4. ^{1}H NMR spectra of HTM_{C6F5} (top) and H_3TD_{C6F5} in $(CD_3)_2CO$ at room temperature.

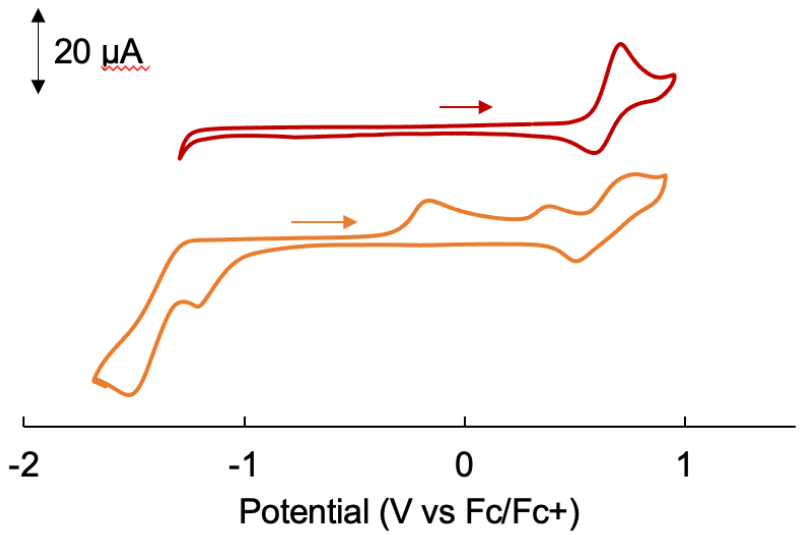

Fig. S5. Cyclic voltammograms of HTM_{C6F5} (red) and H_3TD_{C6F5} (orange) (1.5 mM) at a glassy carbon electrode in CH_2Cl_2 with 0.1 M [(*n*-Bu_4)(PF_6)] as a supporting electrolyte. Data collected at a 100 $mV \cdot s^{-1}$ scan rate using a Ag/AgCl reference electrode and a Pt wire auxiliary electrode.

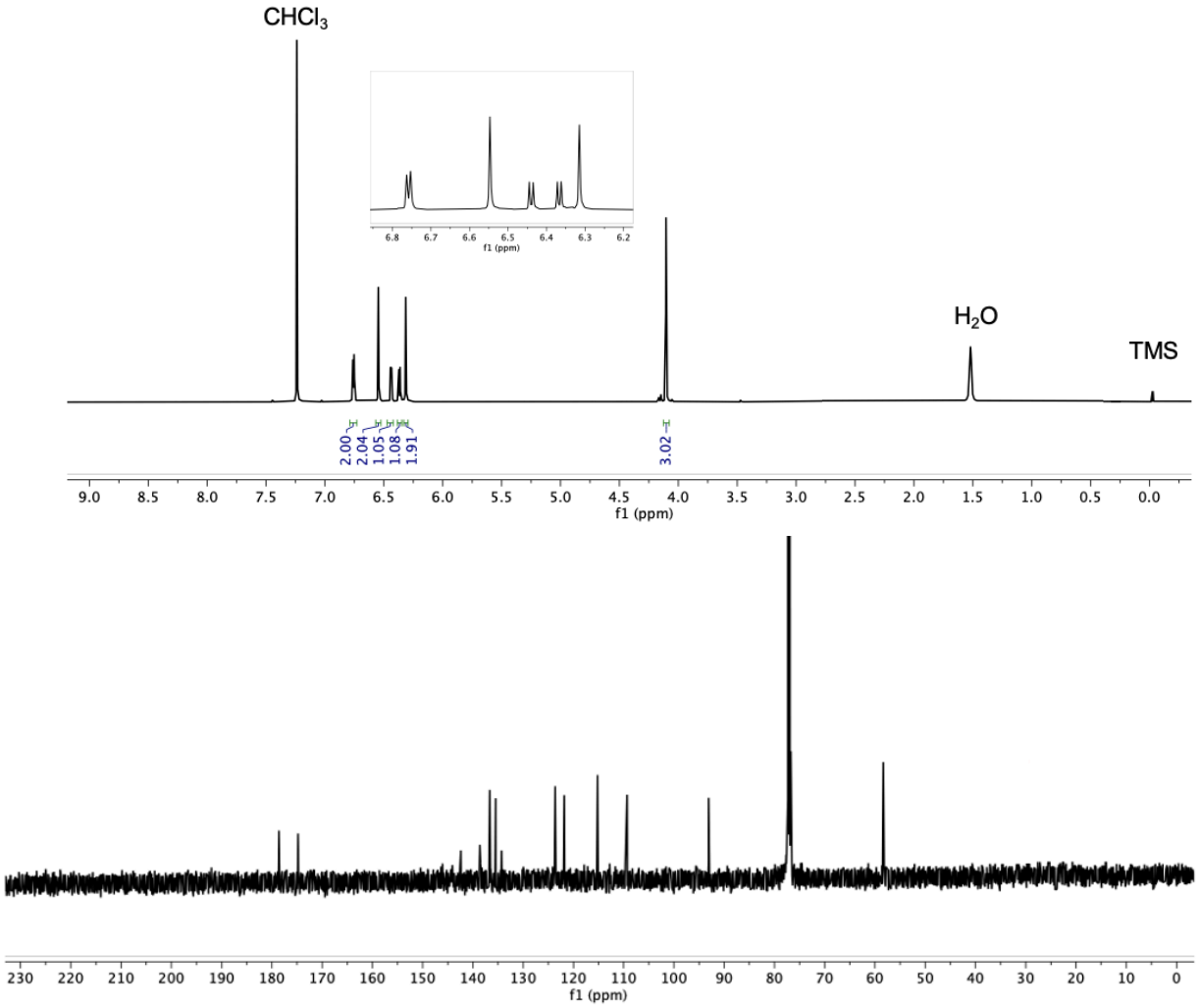

Fig. S6. ^{1}H NMR (top) and ^{13}C NMR (bottom) spectra of [Pd($TM_{C6F5}^{\#}$)] in $CDCl_3$ at room temperature.

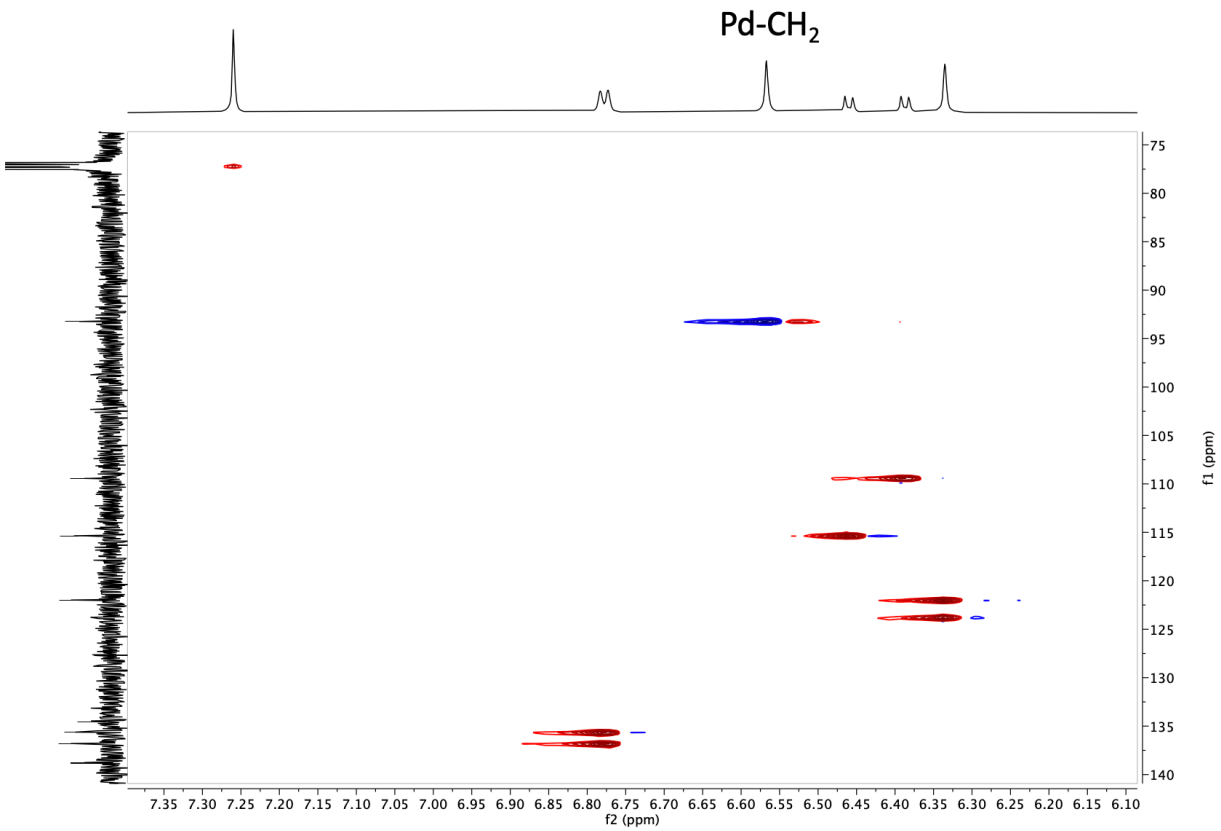

Fig S7. ^{1}H-^{13}C HSQC NMR spectrum of [Pd($TM_{C6F5}^{\#}$)] in $CDCl_3$ at room temperature correlating the methylene carbon at 93.2 ppm to the protons at 6.57 ppm (CH2 peak in blue).

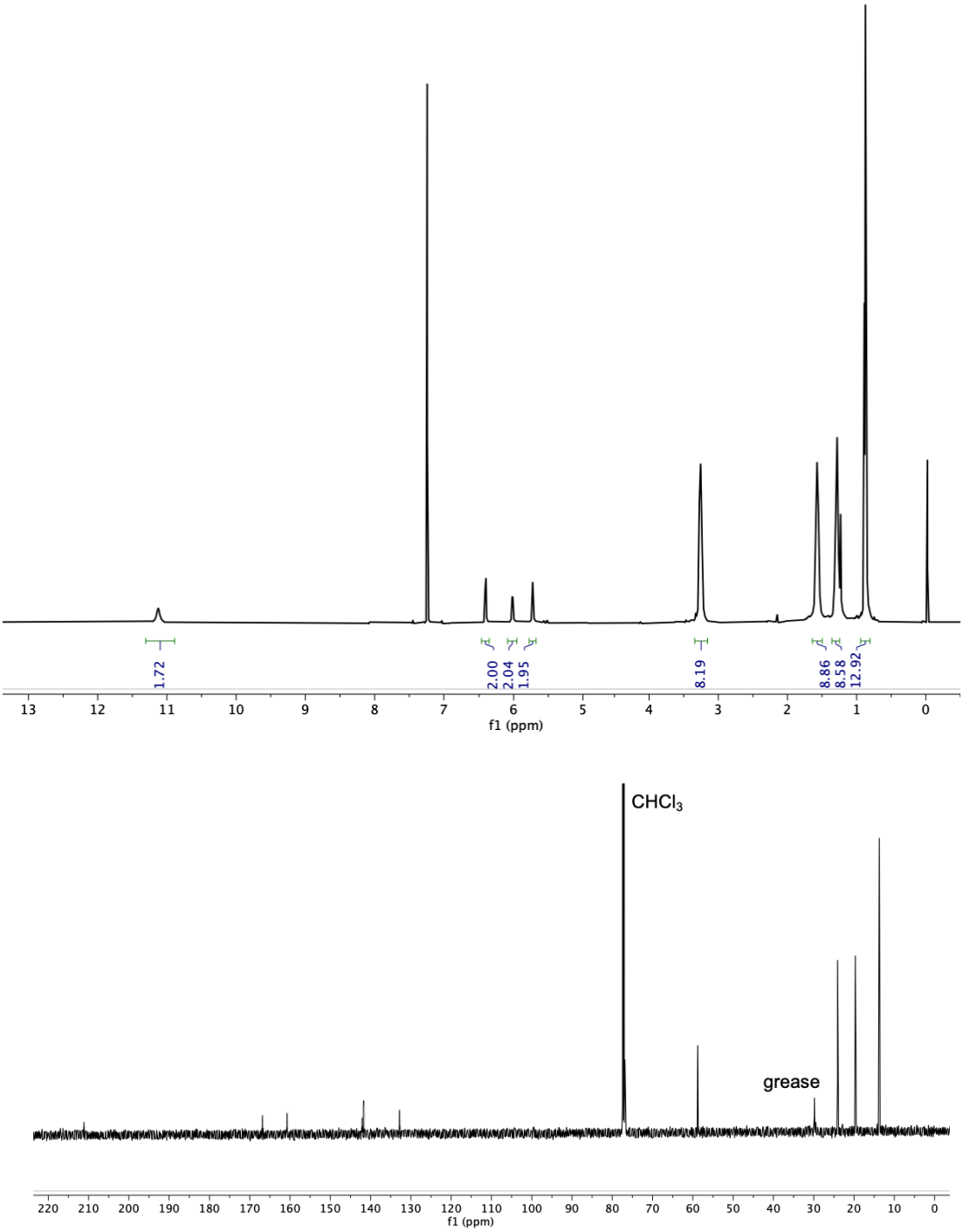

Fig. S8. ^{1}H NMR (top) and ^{13}C NMR (bottom) spectra of [TBA][Pd(TD_{C6F5})(H_2O)] in $CDCl_3$ at room temperature.

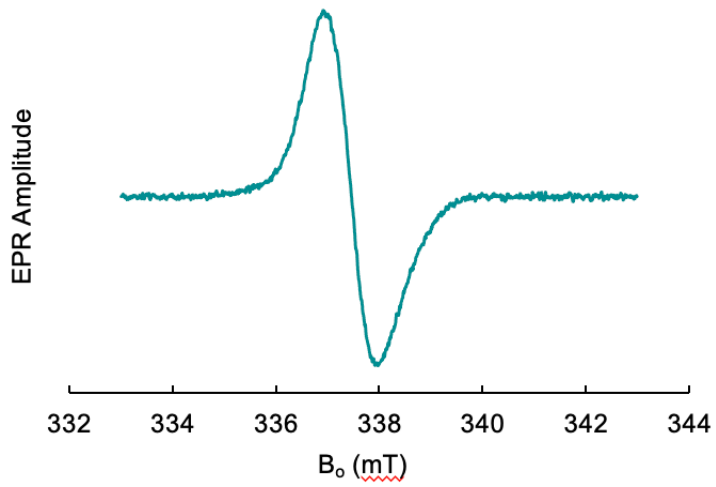

Fig. S9. EPR spectra at 77 K of [Pd(TD_{C6F5}•)(H_2O)]. Experimental conditions: mw frequency, 9.465 GHz, mw power, 5 mW, field modulation amplitude, 0.1 mT.

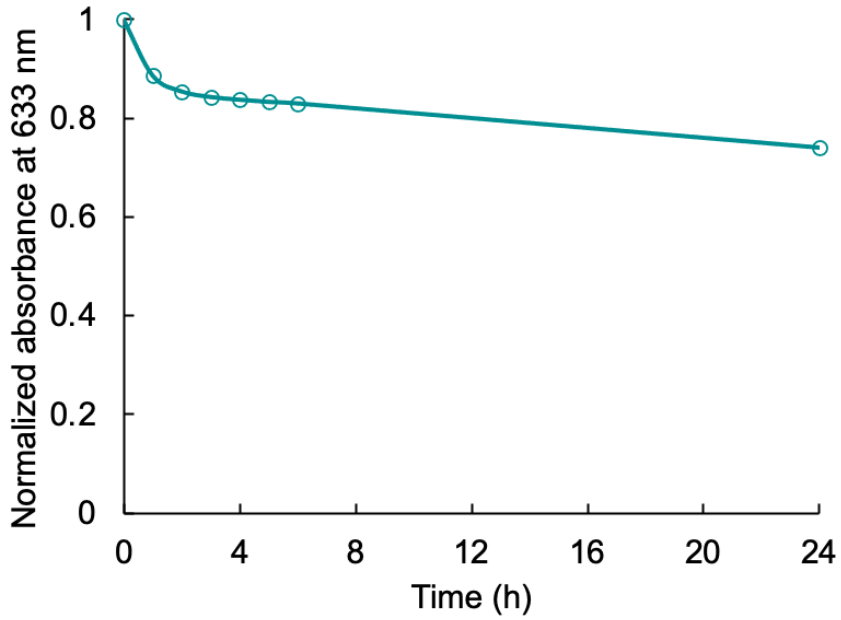

Fig. S10. Stability study of [Pd(TD_{C6F5}•)(H_2O)] in acetone monitored over a course of 24 h.

X-ray diffraction analysis

Data were collected at the University of Arizona Department of Chemistry and Biochemistry X-ray Diffraction Facility. The measurements for HTM_{C6F5} and [Pd($TM_{C6F5}^{\#}$)] were conducted on a Bruker Kappa APEX II DUO diffractometer under the Mo-Kα radiation (λ = 0.71073 Å) generated by a sealed tube and an APEX II CCD area detector. The data sets were collected using the *APEX2* software package (Bruker AXS Inc., Madison, WI, 2007). The measurements for H_3TD_{C6F5} and [TBA][Pd(TD_{C6F5})(H_2O)] were conducted on a using a Bruker Venture D8 MetalJet X-ray diffractometer under gallium Kα rays (λ = 1.34 Å) equipped with a Photon III detector. The data sets were collected using the APEX4 software package. The measurement temperature was 100 K in all cases. The absorption correction was done using a multi-scan method in *SADABS* (Sheldrick, G. M. University of Göttingen, Germany, 1997). The structures were solved in Olex2[1] by the ShelXT program[2] using Intrinsic Phasing and refined with the ShelXL package[3] using least squares minimization. All non-H atoms were located in the Fourier map and refined anisotropically. Carbon-bound hydrogen atoms were calculated in ideal positions, with isotropic displacement parameters set to 1.2U_{eq} of the host atom (1.5U_{eq} for methyl hydrogen atoms). Their positions were then refined using a riding model. Q-peaks for hydrogen-bonded N-H protons were located in the Fourier maps. The corresponding hydrogens were assigned to those positions and refined explicitly. The essential details pertaining to atom assignment, bond lengths, the experiment, and to structure refinement are available in Figures S11-S14 and Tables S1-S2.

Structure refinement of *meso*-pentafluorophenyl α,α'-dimethoxytripyrrin (HTM_{C6F5}). Crystals grew as red-orange plates by slow diffusion of hexane into a solution of CH_2Cl_2 at room temperature. Data collected were optimized for the monoclinic system and the structures were solved in the monoclinic space group $P2_1/c$. The asymmetric unit cell contained two molecules. The highest residual Fourier peak found in the model was +0.81 *e* Å^{-3} approx. 0.92 Å from H8 and the deepest Fourier hole was -0.20 *e* Å^{-3} approx. 1.09 Å from C19.

Structure refinement of meso-pentafluorophenyl-tripyrrindione (H_3TD_{C6F5}). Crystals grew as orange plates by slow diffusion of hexane into a solution of CH_2Cl_2 at room temperature. Data collected was optimized for the monoclinic system and the structures were solved in the monoclinic space group C2/c. The asymmetric unit cell contained four molecules. A B-level alert generated by CheckCif (PLAT097_ALERT_2_B) is caused by the presence of a large reported positive residual density (1.01 e^-/ Å^{-3}) and is not related to any misassigned atom. The highest residual Fourier peak found in the model was +1.51 *e* Å^{-3} approx. 0.97 Å from H7c and the deepest Fourier hole was -0.45 *e* Å^{-3} approx. 0.36 Å from H1d.

Structure refinement of [Pd($TM_{C6F5}^{\#}$)]. Crystals grew as blue plates by slow evaporation the complex in CH_2Cl_2/hexane at RT. Data collected were optimized for the monoclinic system and the structures were solved in the monoclinic space group $P2_1/c$. The asymmetric unit cell contained one molecule. The highest residual Fourier peak found in the model was +0.68 *e* Å^{-3} approx. 0.92 Å from H7 and the deepest Fourier hole was -0.33 *e* Å^{-3} approx. 0.75 Å from Pd1.

Structure refinement of [TBA][Pd(TD_{C6F5})(H_2O)]. Crystals grew as blue plates by slow diffusion of hexane into a solution of acetone at room temperature. Data collected were optimized for the monoclinic system and the structures were solved in the monoclinic space group $P2_1/c$. The asymmetric unit cell contained two complexes. Two large q-peaks were observed in the structure and were presumed to be a small contribution of a twin

since the distances between the peaks matched that of the distance between the palladium centers of the main structures. The twin law in Olex2 was implemented and BASF gave a twinned scale factor of 4.8%. The highest residual Fourier peak found in the model was +2.12 *e* Å^{-3} approx. 0.08 Å from Pd1A and the deepest Fourier hole was –2.81 *e* Å^{-3} approx. 0.48 Å from Pd1.

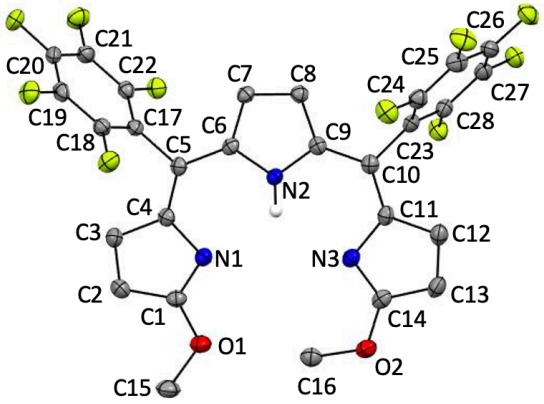

Fig. S11. Labeling scheme for the structure of HTM_{C6F5}. Carbon-bound hydrogens in calculated positions are omitted for clarity. Non-hydrogen atoms are displayed as thermal ellipsoids set at 50% probability level (CCDC 2300776).

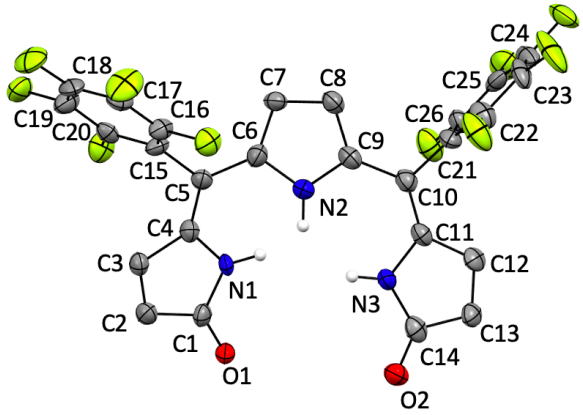

Fig. S12. Labeling scheme for the structure H_3TD_{C6F5}. Carbon-bound hydrogens in calculated positions are omitted for clarity. Non-hydrogen atoms are displayed as thermal ellipsoids set at 50% probability level (CCDC 2300775).

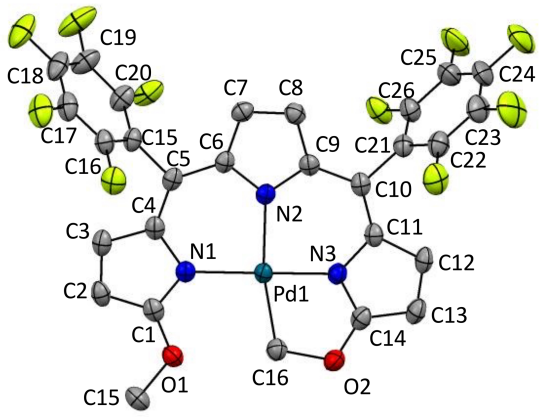

Fig. S13. Labeling scheme for [Pd($TM_{C6F5}^{\#}$)]. Carbon-bound hydrogens in calculated positions are omitted for clarity. Non-hydrogen atoms are displayed as thermal ellipsoids set at 50% probability level (CCDC 2300774).

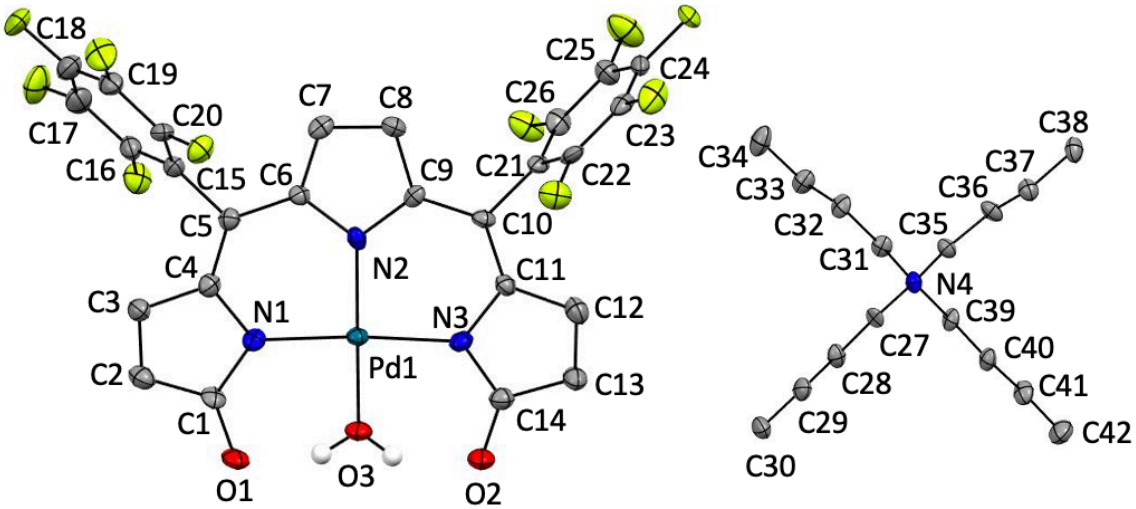

Fig. S14. Labeling scheme for [TBA][Pd(TD_{C6F5})(H_2O)]. Carbon-bound hydrogens in calculated positions are omitted for clarity. Non-hydrogen atoms displayed as thermal ellipsoids set at 50% probability level (CCDC 2300777).

Table S1. Selected bond lengths (Å) in the crystal structures of HTM_{C6F5}, H_3TD_{C6F5}, $[Pd(TM_{C6F5}^{\#})]$, and $[TBA][Pd(TD_{C6F5})(H_2O)]$.

	HTM_{C6F5}	**H_3TD_{C6F5}**	**$[Pd(TM_{C6F5}^{\#})]$**	**$[TBA][Pd(TD_{C6F5})(H_2O)]$**
Pd-N1	---	---	2.037(2)	2.021(9)
Pd-N2	---	---	2.067(2)	2.005(9)
Pd-N3	---	---	1.934(2)	2.019(9)
Pd-X	---	---	C16: 2.035(3)	O3: 2.050(7)
N1-C1	1.309(2)	1.372(9)	1.325(3)	1.393(14)
N1-C4	1.405(2)	1.405(8)	1.404(3)	1.407(14)
N2-C6	1.377(2)	1.368(8)	1.371(3)	1.381(13)
N2-C9	1.374(2)	1.382(9)	1.379(3)	1.387(13)
N3-C11	1.417(2)	1.404(9)	1.388(3)	1.412(14)
N3-C14	1.312(2)	1.372(9)	1.320(3)	1.385(14)
O1-C1	1.334(2)	1.233(8)	1.320(3)	1.269(14)
O1-C15	1.444(2)	---	1.445(3)	---
O2-C14	1.336(2)	1.240(8)	1.307(3)	1.249(14)
O2-C16	1.447(2)	---	1.529(3)	---
C1-C2	1.467(3)	1.465(9)	1.444(4)	1.487(16)
C2-C3	1.347(3)	1.343(9)	1.354(4)	1.358(16)
C3-C4	1.462(3)	1.458(10)	1.446(4)	1.437(16)
C4-C5	1.373(2)	1.360(9)	1.381(4)	1.340(15)
C5-C6	1.443(2)	1.462(9)	1.438(3)	1.425(14)
C6-C7	1.402(2)	1.387(9)	1.417(4)	1.409(15)
C7-C8	1.390(3)	1.403(9)	1.371(4)	1.402(15)
C8-C9	1.406(3)	1.380(9)	1.415(4)	1.400(15)
C9-C10	1.437(3)	1.439(9)	1.441(3)	1.423(14)
C10-C11	1.371(3)	1.366(9)	1.367(4)	1.373(15)
C11-C12	1.460(3)	1.443(10)	1.466(3)	1.433(15)
C12-C13	1.342(3)	1.363(10)	1.350(4)	1.320(16)
C13-C14	1.463(3)	1.462(11)	1.449(4)	1.466(16)

Table S2. Crystal data collection parameters of HTM_{C6F5}, H_3TD_{C6F5}, [$Pd(TM_{C6F5}^{\#})$], and [TBA][$Pd(TD_{C6F5})(H_2O)$].

	HTM_{C6F5}	**H_3TD_{C6F5}**	**[$Pd(TM_{C6F5}^{\#})$]**	**[TBA][$Pd(TD_{C6F5})(H_2O)$]**
Molecular Formula	$C_{28}H_{13}F_{10}N_3O_2$	$C_{26}H_9F_{10}N_3O_2$	$C_{28}H_{11}F_{10}N_3O_2Pd$	$C_{42}H_{44}F_{10}N_4O_3Pd$
Formula Weight [g·mol^{-1}]	613.42	585.36	717.82	949.24
Temperature [K]	100	100	100	100
Crystal Class	Monoclinic	Monoclinic	Monoclinic	Monoclinic
Space Group	$P2_1/c$	C2/c	$P2_1/c$	$P2_1/c$
a [Å]	16.8101(11)	17.9543(18)	15.4778(5)	16.9722(15)
b [Å]	14.7710(11)	17.9220(18)	17.3723(6)	25.354(2)
c [Å]	10.4348(7)	57.541(6)	10.5957(4)	18.9613(17)
α [°]	90	90	90	90
β [°]	106.940(3)	91.715(4)	94.482(2)	102.913(4)
γ [°]	90	90	90	90
Volume [Å]	2478.6(3)	18507(3)	2840.31(17)	7953.0(12)
Z	4	32	4	12
ρ_{calc} [g·cm^3]	1.644	1.681	1.679	1.619
μ [mm^{-1}]	0.156	0.931	0.750	3.558
F(000)	1232.0	9344.0	1408.0	3937.0
Crystal Size [mm]	0.21×0.19×0.06	0.31×0.14×0.02	0.28×0.2×0.08	0.22×0.12×0.04
Measured Reflections	24787	115148	28008	151216
Independent Reflections, I > 2σ[*I*]	4919	16276	5397	151207
R_{int}	0.0354	0.1007	0.0258	0.1465
Goodness-of-fit on F^2	1.018	1.168	1.043	1.059
R_1, $I > 2\sigma[I]$	0.0376	0.1090	0.0286	0.1071
wR_2, all data	0.0969	0.2191	0.0774	0.3185
Peak/hole	0.81/-0.20	1.01/-0.36	0.68/-0.34	2.16/-2.34
CCDC Number	2300776	2300775	2300774	2300777

$R_1 = \Sigma[|F_o| - |F_c|]/\Sigma|F_o|$ $\quad wR_2 = [\Sigma w(F_o^2 - F_c^2)/\Sigma wF_o^4]^{1/2}$

References

1 O. V. Dolomanov, L. J. Bourhis, R. J. Gildea, J. A. K. Howard and H. Puschmann, *OLEX2* : a complete structure solution, refinement and analysis program, *J Appl Crystallogr*, 2009, **42**, 339–341.

2 G. M. Sheldrick, *SHELXT* – Integrated space-group and crystal-structure determination, *Acta Crystallogr A Found Adv*, 2015, **71**, 3–8.

3 G. M. Sheldrick, Crystal structure refinement with *SHELXL*, *Acta Crystallogr C Struct Chem*, 2015, **71**, 3–8.